EVALUATION OF PROGRESS IN CHEMOTHERAPY TREATMENT FOR CHILDHOOD LEUKEMIA PATIENTS USING FTIR MICROSPECTROSCOPY AND CLUSTER ANALYSIS

Jagannathan Ramesh[1], Mahmoud Huleihel[2], Jacov Mordehai[3], Asher Moser[4], Vitaly Erukhimovitch[2], Chen Levi[1], Joseph Kapelushnik[4] and Shaul Mordechai[1©]

[1]Department of Physics, Ben Gurion University, Beer Sheva, 84105, Israel.

[2]Institute of Applied Sciences, Ben Gurion University, Beer Sheva, 84105, Israel.

[3]Department of Pediatric Surgery, Soroka University Medical Center, Beer Sheva, 84105, Israel.

[4]Pediatric Hematology-Oncology, Soroka University Medical Center, Beer Sheva, 84105, Israel.

© denotes the corresponding author : Tel : +972-8-646 1749 ; Fax : 972-8-647 2903

E-mail : shaulm@bgumail.bgu.ac.il

Abstract

Acute lymphoblastic leukemia (ALL) is the most common malignancy in children. Remarkable progress made in the methods of chemotherapy has increased the cure rate to 80%. The leukemic cells called blasts are eliminated within seven days of chemotherapy treatment. Clinically, the blast count is monitored directly using blood smears by the specific genetic markers and immunophenotyping methods such as flow cytometry. In this article, we present a novel approach to monitor the progress made due to chemotherapy in one B and two T cell ALL child patients using recent novel optical method called FTIR-microspectroscopy (FTIR-MC) and cluster analysis. Our results indicated that the biological marker derived from the spectra could not provide accurate prediction of the progress made due to chemotherapy. However the simple cluster analysis of FTIR spectra provided good classification of the samples with and without blasts, which correlate satisfactorily with clinical data. This report is an example of the potential application of FTIR-MC in the diagnosis and follow-up of various types of malignancies.

Keywords : ALL ; Chemotherapy ; blast ; FTIR Microspectroscopy ; biological markers ; Cluster analysis

1.Introduction

Acute lymphoblastic leukemia (ALL) is the most prevalent type of malignancy accounting for 33% among children (1). The aetiology of ALL in children is understood in some detail[2]. Genetic changes in hemopoietic cells lead to ALL which is a clonal hematological disorder arising due to [3]. The translocations of MLL gene occur in 80% cases of ALL [4]. Current rate of cure is nearly 80% in children (5) whereas it is only 30-40% in adults (6) The successful cure of childhood ALL can be attributed to striking progress made in chemotherapy procedures. The malignant B or T cells present in the peripheral lymphocytes isolated from the patient are called as blasts. Blast count in patients is monitored by physicians using variety of techniques (7). Even a single blast can be detected by minimal residual disease assessment (8). Cocktail of drugs such as doxorubicin, methotrexate (MTX), L-aspartase and Ara-c decrease the blast count dramatically within a week of treatment (9).

In chemistry and biology, the role of FTIR has been the characterization, guiding the chemists and revealing the biomolecular structure for biologists (10,11). Last few years has witnessed the application of FTIR in medicine. Even though the use of FTIR in clinics is far from reality, the initial efforts in the diagnosis of cancer (12,13,14) and other disorders (15) are certainly encouraging and demands extensive study. FTIR characterization of chronic lymphoblastic leukemia (16) (CLL) and the effect of anti-leukemia drugs on leukemia cells *in vitro* have been reported (17). In this report we present a novel approach to evaluate the progress made due to chemotherapy in ALL child patients using FTIR Microspectroscopy (FTIR-MC) and cluster analysis. Our

preliminary results indicated that results obtained from FTIR-MC and cluster analysis correlate satisfactorily with clinical data.

2 Materials and Methods

2.1 Isolation of cells and sample preparation

Blood samples were collected from three children admitted in Soroka University Medical Center (SUMC) (one B cell and two T cell ALL patients) with their consent. Standard chemotherapy treatment protocol (BFM 95) was administered for all patients. Blast count was performed using cytogenetic methods and flow cytometry techniques. The blood was processed within two hours for the isolation of the lymphocytes. Lymphocytes were isolated as previously described [18]. The processed samples containing mononuclear cells were checked for residual RBC (Red Blood Cells) contamination.

2.2 FTIR Microspectroscopy and Cluster analysis

Mononuclear cells were loaded on Zinc-Selenium (ZnSe) crystals and later air dried completely. FTIR data were collected using modern FTIR microscope (BRUKER EQUINOX model 55/S OPUS software). Measurement site covered 50 μm diameter and the spectra taken were average of 128/256 scans to increase the signal to noise ratio. The resolution was 4 cm^{-1} and ten different measurements were made for each sample. The spectra with high signal to noise ratio (≥1000) were used for further data analysis. ORIGIN software was used for calculating the integrated absorbance and the error bars represent the maximum SD obtained in all of our measurements. Cluster analysis was

performed with good quality spectra having high signal to noise ratio. The spectra of day zero (the day before the treatment begun) and first seven days of chemotherapy treatment were used for cluster analysis. The Ward's minimum variance method was used for the cluster analysis, which was provided in the OPUS software.

3 Results

3.1 Blast count

The percentage of blast counts in both B and T cell patients determined by flow cytometry and microscopic inspection is shown in Figure 1. For B cell patient, blast percentage, which was initially 85% reduced dramatically on chemotherapy treatment and finally the blast percentage was nearly to zero on the 7^{th} day of treatment in the peripheral blood. In the case of T1 cell patient, blast percentage was reduced to zero on the 3^{rd} day of treatment and maintained till the 5^{th} day in peripheral blood. In another T2 patient, the blast count, which was initially 86%, reduced to 20% after two days of chemotherapy. Further treatment led to decrease in blast percent and finally it was observed to be zero on the 7^{th} day of treatment.

3.2 FTIR Microspectroscopy

a) B Cell ALL Patient

Figure 2a shows the FTIR-MC spectra (average of ten measurements) of day zero (before the chemotherapy treatment) and days 2 and 7 of the treatment from a B cell ALL patient. Interesting results were obtained during the first seven days of chemotherapy treatment. The decrease in absorbance was observed for the 2^{nd} day of the chemotherapy

treatment in the region between 950-1500 cm^{-1} compared to day zero. As the treatment continued for a week, there was significant reduction in the absorbance observed on day 7 of the treatment. The absorbance changes were in good correlation with blast percentage for B cell patient. The second derivative spectra for day zero and seven are shown in Figure 2b. Minima at 965, 1080 and 1100 cm^{-1} showed significant changes in intensity and frequency shifts were also observed in the region between 1400-1500 cm^{-1}. No significant absorbance changes were observed with treatment in the higher wavenumber region (2600-3600 cm^{-1}) of the spectrum.

b) T1 Cell ALL Patients

FTIR-MC spectra of mononuclear cells isolated from control, day zero, 3rd and 7th day of chemotherapy treatment for the T1 cell patient is presented in Figure 3a. Absorbance changes were observed only in the region between 1200-1600 cm^{-1} for control and day zero of T1 cell patient. It was significant with amide II peak compared to phosphate absorbing regions of the spectrum (1000-1200 cm^{-1}). Interestingly, the shoulder around 1050 cm^{-1} broadened for days 3 and 7 of treatment. Intensity differences were observed with a small IR band at 965 cm^{-1} arising due to symmetric stretching vibrations from phosphodiester bonds of the nucleic acids (19). Second derivative spectra for day zero and third day of treatment are shown in the Figure 3b. Notable frequency shifts (± 2-6 cm^{-1}) were observed in the regions such as 1000-1100 and 1400-1550 cm^{-1}. The frequency shifts were considerably larger in magnitude for the T1 cell case than the B cell patient.

c) T2 cell ALL patient

FTIR-MC spectra for the T2 cell ALL patient is presented in the Figure 4a. Spectral changes due to seven days of chemotherapy were similar to the B cell ALL patient shown in the Figure 4a. Dramatic decrease in absorbance was observed in the phosphate absorbing regions (1000-1300 cm^{-1}) after seven days of chemotherapy treatment. No significant absorbance changes were observed with amide II peak on chemotherapy treatment. As in the case of T1 patient, the second derivative spectra shown in Figure 4b indicated that the frequency shifts observed in the 1000-1100 and 1400-1550 cm^{-1} regions were lower in magnitude (not more than 3 cm^{-1}) compared to the T1 cell ALL patient. T2 cell patient showed no notable differences in the absorbance with chemotherapy treatment in the region between 2600-3600 cm^{-1}.

3.3 Biological Marker derived from IR Spectra

a) RNA/DNA

Andreus et.al reported that the grading of lymphoid tumor could be achieved by the ratio of RNA/DNA at 1121/1020 (20). In our case, the percentage of blasts can be considered equivalent to the stage of the disease. Administration of cocktail of drugs would be expected to lower the severity of the disease. Results on RNA/DNA at1121/1020 for B and T cell ALL patients are given in Figure 5 a, b & c. In all the cases, day –1 represents the average of four healthy controls. In the case of B cell ALL patient, first day treatment led to a slight increase in RNA/DNA and later decreased with discrete fluctuations till 10^{th} day of treatment. Saturation was observed from 10-16 days. The T1 cell ALL case showed a sharp decline in RNA/DNA reaching the lowest value on 3^{rd} day

of treatment in agreement with the blast count. Further increase was observed from 3-11 days and later stabilized. In the case of T2 (Figure 5c), RNA/DNA decreased in the first two days of treatment and the fluctuations were observed between second and fifth day. Later, steady decrease was observed from 5-9 days of treatment.

3.4 Cluster analysis

a) B cell ALL Patient

Figure 6a shows the dendrogram obtained from cluster analysis results of the FTIR-MC spectra in the region between 999-1151 cm^{-1}, which include the spectra from day zero to nine for the B cell ALL patient. Day zero having 85% blast and the seventh day (after treatment) were grouped into two different clusters. The major cluster had two sub-clusters having 0-2 days and days 5,6 and 9. Analysis of the region between 1178-1302 cm^{-1} (Figure 6b) showed two major clusters, giving rise to clear separation of day zero and day seven. In the second major cluster (bottom), day 6 with blast count between 10-20% had higher heterogeneity compared to days 7-9 where the blasts were completely absent. Inclusion of the above regions from 999-1302 cm^{-1} (Figure 6c) shows that the day zero and seven are still separated with lower heterogeneity compared to the region between 1178-1302 cm^{-1}. The major cluster had two sub-clusters similar to the major cluster shown in Figure 6a. Cluster analysis of the spectra in the region 2798-3001 cm^{-1} showed a major cluster with poor classification of treated and untreated samples (data not shown).

b) T1 cell ALL Patient

The dendrograms obtained on the cluster analysis of FTIR-MC spectra of mononuclear cells from the first T cell ALL patient (T1) is presented in Figure 7 a-c. The region in the spectra taken for analysis between 999-1151 cm^{-1} showed major and minor clusters. In the minor cluster, day zero and ten were mixed showing poor separation between treated and untreated samples. The major cluster had two sub-clusters where day one and three with high heterogeneity among the other treatment samples. The results of the cluster analysis for spectral window in the region 1178-1302 cm^{-1} are presented in Figure 7b. The major cluster could not classify the spectra for day zero and the other treatment samples. The cluster analysis of spectral window in the higher wavenumber region between 2798-3001 cm^{-1} (shown in Figure 7c) provided good classification of day zero-one and other treatment samples after three days of chemotherapy treatment. The major cluster in the dendrogram had all the spectra where no blasts were found in the patient's blood samples.

c) T2 cell ALL Patient

Cluster analysis of the FTIR-MC spectra in different regions are shown in Figure 8 a-c for the second T cell ALL patient (T2). Symmetric and asymmetric stretching regions of phosphate provided good classification between the samples with and without blasts. Days 0-1 and 5-9 formed two major clusters having high heterogeneity between them. Cluster analysis in the region between 2600-3600 cm^{-1} (data not shown) performed poorly giving rise to mixing of treated and untreated blasts for the T cell ALL patients (T1 and T2).

4 Discussion

With the advancement made in the methods of chemotherapy, cure rate for ALL in children is closer to 80%. Generally most of the anti-cancer drugs act by interfering with the nucleic acids synthesis or their function (21). For example, doxorubicin interchelates into the DNA and induces topoisomerase –mediated single and double stranded breaks in DNA (22). Methotreate (MTX) inhibits the enzyme dihydrofolate reductase (DHFR) thereby depleting the building blocks of DNA (23). L-asparginase has a selective anti-leukemic effect reducing the L-asparagine (L-Asn) concentration in the blood (24). Normal cells respond to the depletion of L- Asn by enhancing the L-Asparagine synthase activity. In contrast, the leukemic cells have low levels of this enzyme leading to starvation of this essential aminoacid. Even though genetic abnormalities are found in both B and T cell ALL patients, the prognostic and therapeutic implications are more pronounced in B cell ALL cases (25). The specific translocations in B cell patients have an increased risk of treatment failure than the T cell patients.

The spectral changes for B cell ALL were significant in the phosphate metabolites absorbing regions between 1000-1300 cm^{-1} for day zero and seven which correspond to 85% and zero percent blast count achieved after the chemotherapy treatment. More than two fold decrease in the absorbance was observed between day zero and seven in the region between 1000-1300 cm^{-1}. This decrease might be due to the dramatic changes in the nucleic acid content in the cells due to the administration of anti-leukemic agents. But, in the case of T cell ALL case, the absorbance changes were not as dramatic as for B cell case. Significant changes in intensity were observed in the region between 1350-

1500 cm^{-1}. The spectral changes might arise due to percentage of blast count before chemotherapy and patient's response to the chemotherapy treatment. These observations suggest that FTIR spectra could offer some clues into the progress made due to chemotherapy in ALL patients.

Quantification of selected biological markers derived from the FTIR-MC spectra provided their usefulness in monitoring the chemotherapy treatment. DNA marker amide I/II was not a sensitive marker as the percent change before treatment and the day on which blasts completely disappeared was not significant (data not shown). For B and T cell ALL the percent changes were 27 and 13 respectively. The decreasing trend reached the minimum on 8^{th} and 10^{th} day for B and T1 cell cases. Another nucleic acid marker RNA/DNA fluctuated from 5-12 days of treatment for B cell ALL suggesting that it is not a suitable marker for this purpose. Contrary to B Cell ALL, RNA/DNA for the T cell patients had local minima on the 3^{rd} day of treatment where the blasts count reduced to zero percent. In addition, percentage change between day zero and three was 47, which was higher than the B cell ALL case. Among the biological markers, RNA/DNA performed better in the case of T1 cell ALL patient. Even though RNA/DNA was found to be decreasing on treatment in T2 cell ALL patient, it was a poor indicator of the progress made due to the therapy due to the fluctuations observed between 2-5 days.

Cluster analysis was performed to classify the samples with and without blasts to give clues on the effect of chemotherapy within the first seven days of treatment. In the case of B cell ALL, the cluster analysis of spectral regions 999-1151 and 999-1302 cm^{-1}

(Figure 6 a and c) clearly classified the samples with and without blasts unambiguously. In addition, the effect of anti-leukemic agents could be understood from the fact that the presence of two sub-clusters (B0, B1, B2 and B5, B6 B9) grouped with samples having high and low blast count respectively. Best results were obtained by the cluster analysis of the spectral region 1178-1302 cm^{-1} where two major clusters representing high and no blast status with the exception of sample B6. Sample B6 had heterogeneity of 0.35 while the other three samples (B7, 8, 9) formed a major sub-cluster indicating a sharp difference in their biomolecular contents. The spectral region between 1178-1302 cm^{-1} is due to the asymmetric stretching vibration arising from the phosphate group containing metabolites. In the case of T cell ALL (T1), cluster analysis (Figure 7) of spectral region 999-1151 and 1178-1302 cm^{-1} did not provide good classification of samples with or without blasts. However, analysis of spectral region between 1178-1302 cm^{-1} indicated that the largest heterogeneity value was obtained for T10 sample compared with respect to other samples. The spectral region between 2798-3001 cm^{-1} corresponding to asymmetric stretching vibration of CH2 and CH3 groups from proteins, phospholipids and nucleic acids provided reasonably good classification between the two groups. Among the no blasts samples, T10 had the high heterogeneity value with other samples. Spectroscopically, the real effect of chemotherapy was observed on 10^{th} day, which differs from clinical data. The results obtained for T2 cell ALL patient were similar to the B cell ALL case giving good classification with either symmetric or asymmetric stretching regions of the phosphate group. In addition, both cases (B and T2) showed poor classification with high wavenumber region (2798-3001 cm^{-1}). It is important to note that our cluster analysis results showed good correlation with the blast count

determined by biochemical methods. At present, the minimal residual disease is evaluated by PCR technique, which is highly sensitive, and expensive compared to the approach outlined in this report. The isolation of B or T cells from total mononuclear cells is expected to improve the sensitivity of our method. Nevertheless, we strongly hope that the use of optical methods will be indispensable in achieving the goal of objectivity in the diagnosis and follow-up for various types of malignancies in the future.

5 Summary and Conclusions

FTIR-MC spectra of mononuclear cells obtained from B cell ALL patient indicated that there were significant differences in the absorbance in the region of phosphate group. These absorbance changes may correspond to the reduction in nucleic acids synthesis in the cells due to chemotherapy. In the case of T cell, absorbance changes were observed in the amide II peak with treatment. Frequency shifts were also observed with T cell ALL compared to B cell ALL case. The biological marker RNA/DNA also declined with treatment for both B and T cell ALL and the rate of decrease was higher for the later. The biological marker reported in this study was not very sensitive to the elimination of blasts present in the blood sample during the treatment. Cluster analysis showed good classification of samples with and without blasts emphasizing the importance of medical informatics. For B and T2 cell ALL, the spectral region between 1178-1302 cm^{-1} was the best giving **a** clear picture of the effect of anti-leukemic agents. In the case of T1 cell ALL, the higher wavenumber region between 2798-3001 cm^{-1}, which corresponds to the asymmetric stretching vibration of CH2, and CH3 groups from the essential biomolecular components of the cell was proved to be the

successful region. This study is an encouraging step for the combined use of combination of optical method and mathematical tools in the field of diagnosis and follow-up of certain types of malignancies.

Acknowledgements

This research work was supported by the Israel Cancer Association (ICA), Israel Science Foundation (ISF Grant No : 788/ 01), and the Harry Stern Applied Research Grant Program. Many thanks are due to Dr. B. Cohen for fruitful discussions. We also thank Mrs. Marina Talyshinsky for technical support during this work.

References

1. J. E. Rubnitz, and Ching-Hon Pui, "Recent advances in the biology and treatment of childhood acute lymphoblastic leukemia," Current Opinion in Hematology. 4, 233-241 (1997).

2. M. F. Greaves, "Aetiology of acute leukemia," Lancet. 349, 344-349 (1997).

3. C. A. Felix and B. J. Lange, "Leukemia in Infants," The Oncologist. 4, 225-240 (1999).

4. P.H. Sorensen, C.S. Chen, F.O.Smith, D.C. Arthur, P.H. Domer, I.D. Berstein, S.J. Korsmeyer, G.D. Hammond and J.H. Kersey, **"**Molecular rearrangements of the MLL gene are present in most cases of infant acute myeloid leukemia and are strongly correlated with monocytic or myelomonocytic phenotypes," J. Clin. Invest 93, 429-437 (1994).

5. C-H. Pui, "Acute leukemia in children," Curr. Opin. Hematol. 3, 249-258 (1996).

6. C-H. Pui and W. E. Evans, "Acute lymphoblastic leukemia," Drug Therapy 339, 605-613 (1998).

7. A. Wakita, M. Nitta, Y. Mitomo, M. Takahashi, M. Tanaka amd T. Kaneda, "Flow cytometric detection of proliferative cells in leukemias," Jpn. J. Cancer. Res 85, 204-210 (1994).

8. G. Nick, "Practical application of minimal residual disease assessment in childhood acute lymphoblastic leukemia," Br. J. Haematol 112, 275-281 (2001).

9. J.F. Margolin and D.G. Poplack, "Acute lymphoblastic leukemia," In A.P.Philip and G.P.David, editors. "Principles and practice of Pediatric oncology," PA: Lippincott-Raven publication, 433-460 (1997).

10. B. Schrader (ed), "Infrared and Raman spectroscopy," VCH publication, Germany (1995).

11. Mantsch, HH and Chapman, D (1996) (eds.), Infrared Spectroscopy of Biomolecules, (chapters 2, 6, 7, 8, 9) John Wiley, N.Y.

12. M.A Cohenford and B. Rigas, "Cytologically normal cells from neoplastic cervical samples display extensive structural abnormalities on IR spectroscopy : implications for tumor biology," Proc. Natl. Acad. Sci USA. 95, 15327-15332 (1998).

13. S. Argov, J.Ramesh, A. Salman, S. Igor, J.Goldstein, H.Guterman and S.Mordechai, "Diagnostic potential of FTIR Microspectroscopy and advanced computational methods in colon cancer patients," J. Biomed. Opt (In Press).

14. R. K. Dukor, M. N. Liebman and B. Johnson, "A new non-destructive method for analysis of clinical samples with FTIR-microspectroscopy. Breast cancer as an example," Cell. Mol. Biol 44, 211-217 (1998).

15. L.-P. Choo, J. R. Mansfield, N. Pizzi, R. L. Somorjai, M. Jackson, W. C. Halliday and H. H. Mantsch, "Infrared spectra of human central nervous system tissue : Diagnosis of Alzheimer's disease by multivariate analysis," Biospectroscopy 2, 141-148 (1995).

16. C.P. Schultz, K. Liu, J. B.Johnston and H. H. Mantsch, "Study of chronic lymphocytic leukemia cells by FT-IR spectroscopy and cluster analysis," Leuk. Res 20, 649-655 (1996).

17. K-Z. Liu, C. P. Schultz, J. B. Johnson, K. Lee and H. H. Mantsch, "Comparison of infrared spectra of CLL cells with their *ex vivo* sensitivity (MTT assay) to chlorambucil and cladribine," Leuk. Res. 21, 1125-1133 (1997).

18. L. Hudson and F. C. Poplack, "Practical immunology," Blackwell publication, London (1976).

19. M. Diem, S.Boydston-White. and L. Chiriboga L, "Infrared spectroscopy of cells and tissues: Shining light onto a novel subject," Applied Spectroscopy, 53 148-161, (1999).

20. P.G. Andreus and R.D. Strickland, "Cancer grading by Fourier transform infrared spectroscopy," Biospectroscopy, 4, 37-46 (1998).

21. J. F. Margolin and D. G. Poplack, "Acute lymphoblastic leukemia,". In Philip, A.P., David, G.P., editors. "Principles and practice of Pediatric oncology," PA: Lippincott-Raven publication, 433-460, (1997).

22. G. N. Hortobagyi, "Anthracyclines in the treatment of cancer. An overview," Drugs. 54 (4), 1-7 (1997).

23. G. S. Longo-Sorbello and J. R. Bertino, "Current understanding of methotrexate pharmacology and efficacy in acute leukemias. Use of newer antifolates in clinical trials," Hematologica. 86 (2), 121-127 (2001).

24. H. J. Müller and J. Boos, "Use of L-asparaginase in childhood ALL," Crit. Rev. Oncol. Hematol. 28 (2), 97-113 (1998).

25. C. A. Felix and B. J. Lange, "Leukemia in infants," The Oncologist. 4, 225-240 (1999).

Figure Captions

Figure 1 : Percentage of blasts for B and T cell ALL patients. Data was obtained by using flow cytometry and cytogenetic methods.

Figure 2 (a) FTIR-MC spectra of B cell ALL patient at different days. I) zero II) Two III) seven. The spectra shown in Figures 2a-4a were normalized to the amide I peak. b) Second derivative spectra I) With blasts (day zero) III) without blasts (day seven) for B cell ALL patient.

Figure 3 (a) FTIR-MC spectra of T cell (T1) ALL patient at different days I) zero II) one III) three. b) Second derivative spectra I) With blasts (day zero) III) without blasts for T cell ALL patient (T1).

Figure 4 (a) FTIR-MC spectra of T cell (T2) ALL patient at different days I) zero II) one III) seven. b) Second derivative spectra I) With blasts (day zero) III) without blasts for T cell ALL patient (T2).

Figure 5 : RNA/DNA is shown as the ratio of absorbance at 1121/1020 cm^{-1}.
a) B cell ALL b) T1 cell ALL c) T2 cell ALL patients.

Figure 6 : Dendrogram presentation for the cluster analysis of FTIR-MC spectra performed in the different regions for B cell ALL patient at different days after

treatment. Each member of the cluster is denoted by cell type (B or T) and the day of treatment. Day zero stands for the day of admittance to the medical center.

a) 999-1151 b) 1178-1302 c) 999-1302 cm^{-1}. Cluster analysis was performed with baseline corrected and amide I normalized spectra.

Figure 7 : Dendrogram presentation for the cluster analysis of FTIR-MC spectra performed in different regions for T1 cell ALL patient at different days. a) 999-1151 b) 1178-1302 c) 2798-3001 cm^{-1}.

Figure 8 : Dendrogram presentation for the cluster analysis of FTIR-MC spectra performed in different regions for T2 cell ALL patient at different days.

a) 999-1302 b) 1178-1302 c) 1178-1281 cm^{-1}.

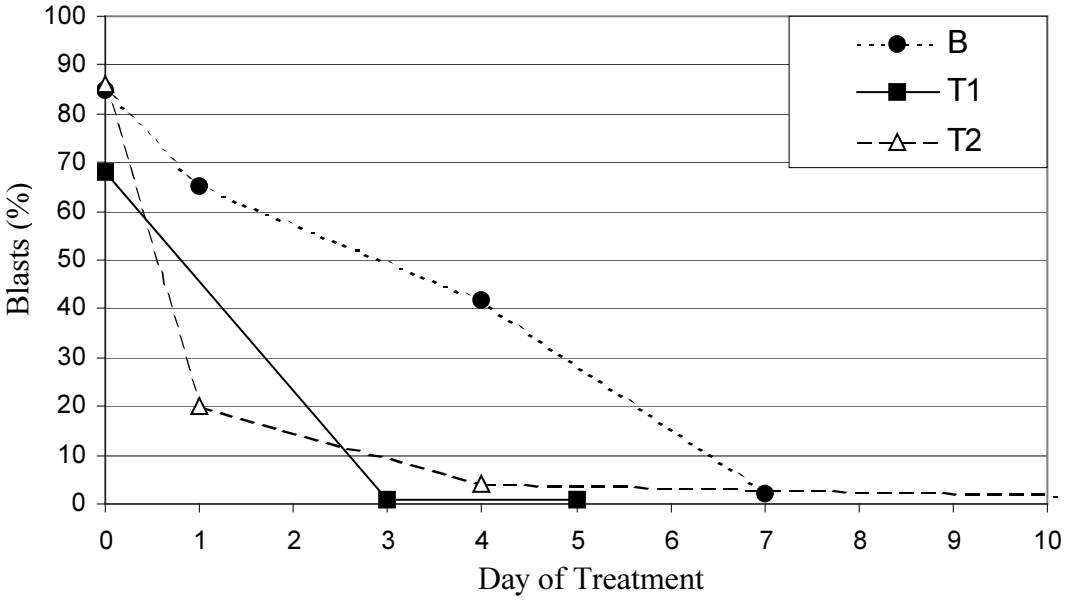
100
90
80
70
60
50
40
30
20
10
0
Blasts (%)
0
1
2
3
4
5
6
7
8
9
10
Day of Treatment
B
T1
T2

Fig. 1

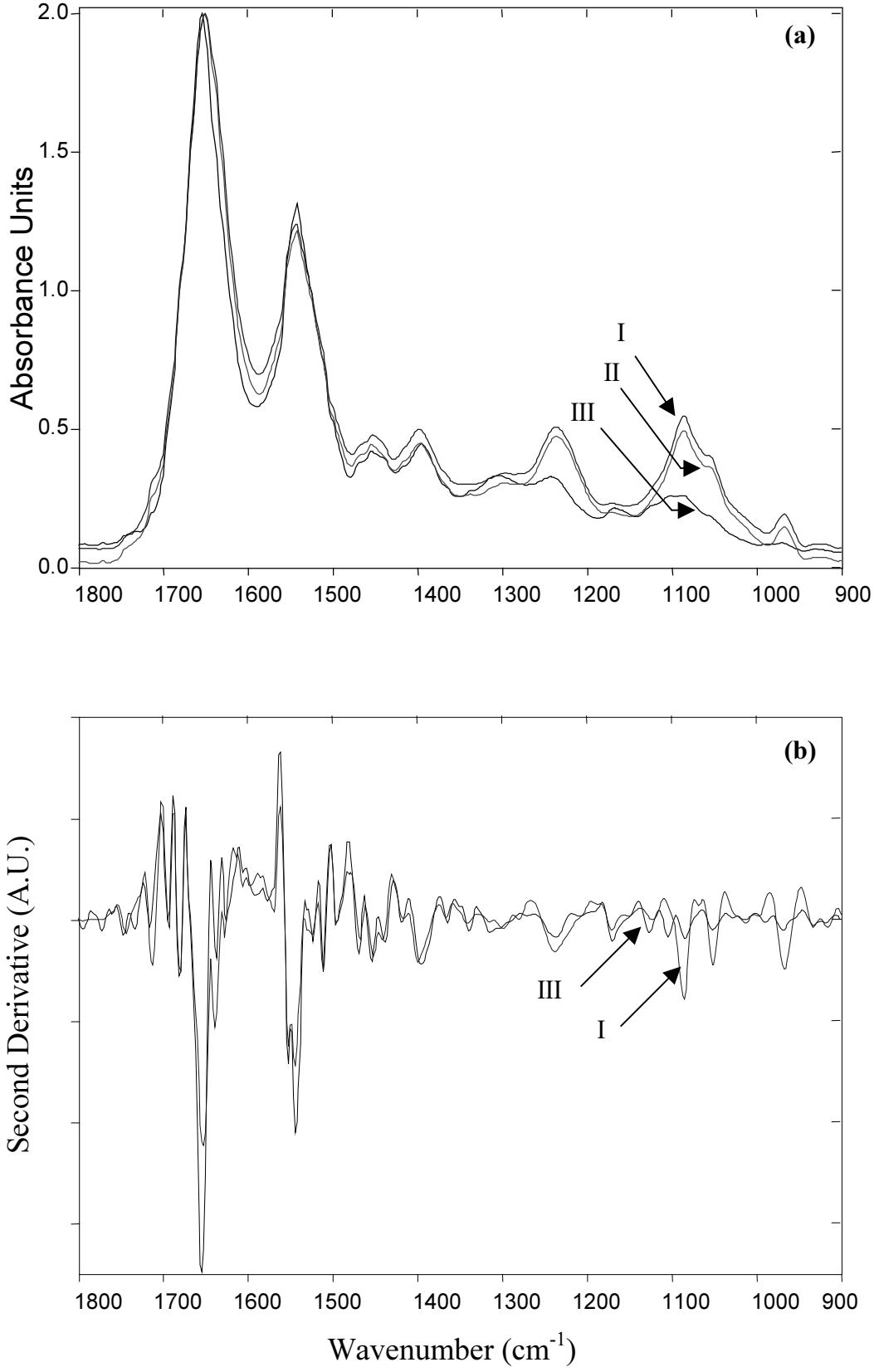
(a)
Absorbance Units
2.0
1.5
1.0
0.5
0.0
I
II
III
1800
1700
1600
1500
1400
1300
1200
1100
1000
900
(b)
Second Derivative (A.U.)
III
I
Wavenumber (cm-1)

Fig. 2

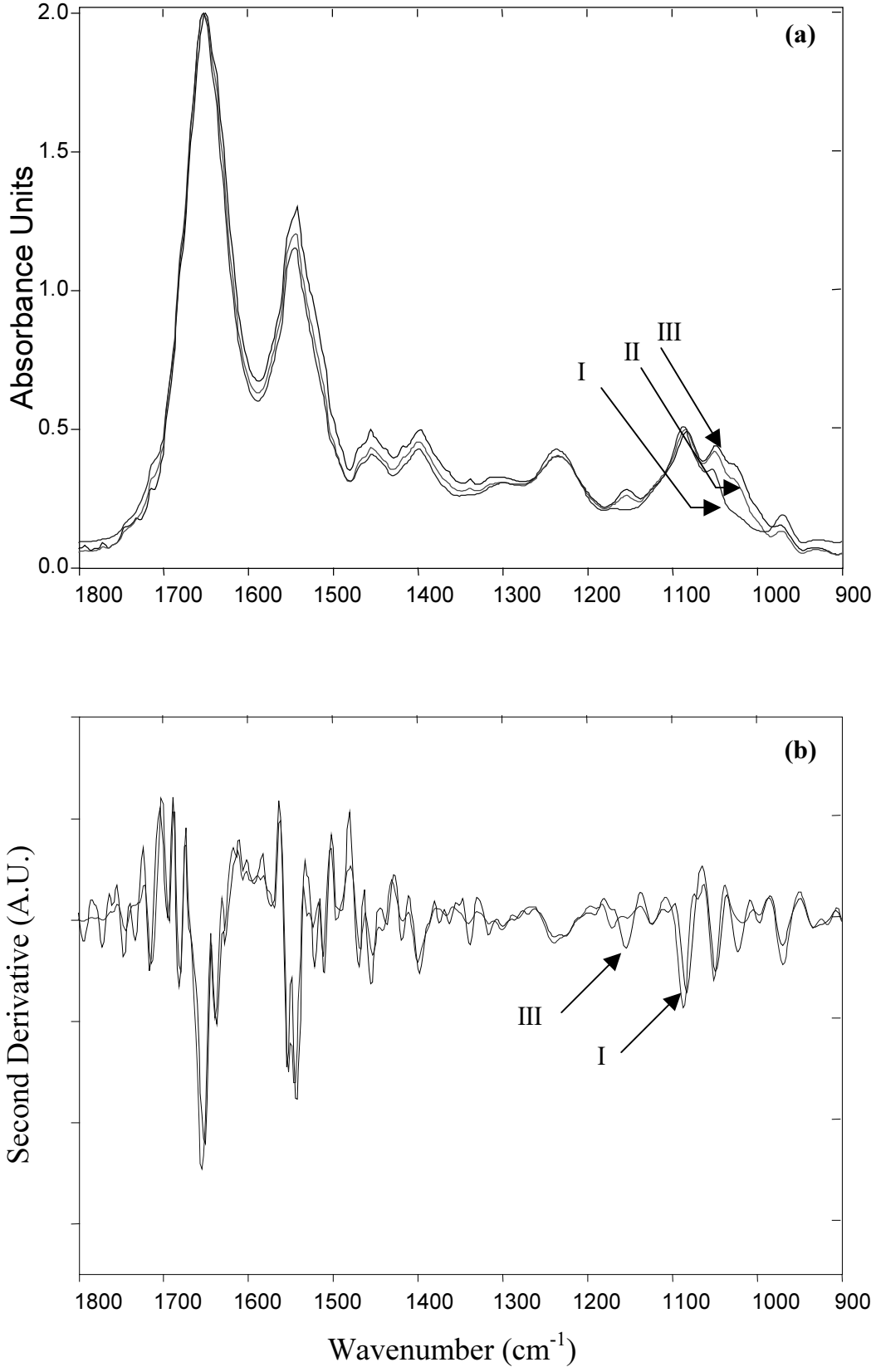
(a)
Absorbance Units
2.0
1.5
1.0
0.5
0.0
I
II
III
1800
1700
1600
1500
1400
1300
1200
1100
1000
900
(b)
Second Derivative (A.U.)
III
I
Wavenumber (cm-1)

Fig. 3

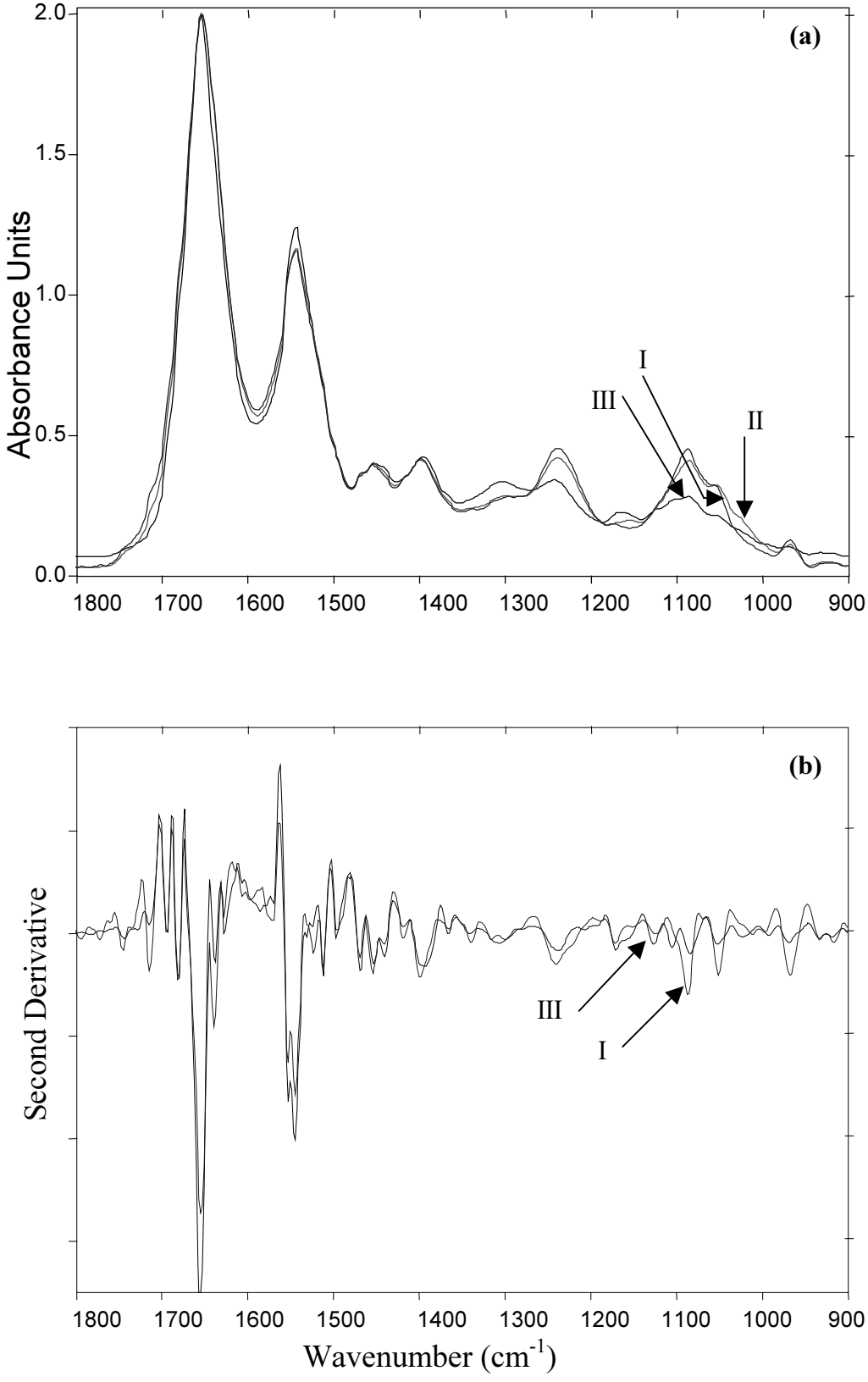
(a)
Absorbance Units
2.0
1.5
1.0
0.5
0.0
I
III
II
1800
1700
1600
1500
1400
1300
1200
1100
1000
900
(b)
Second Derivative
III
I
Wavenumber (cm-1)

Fig. 4

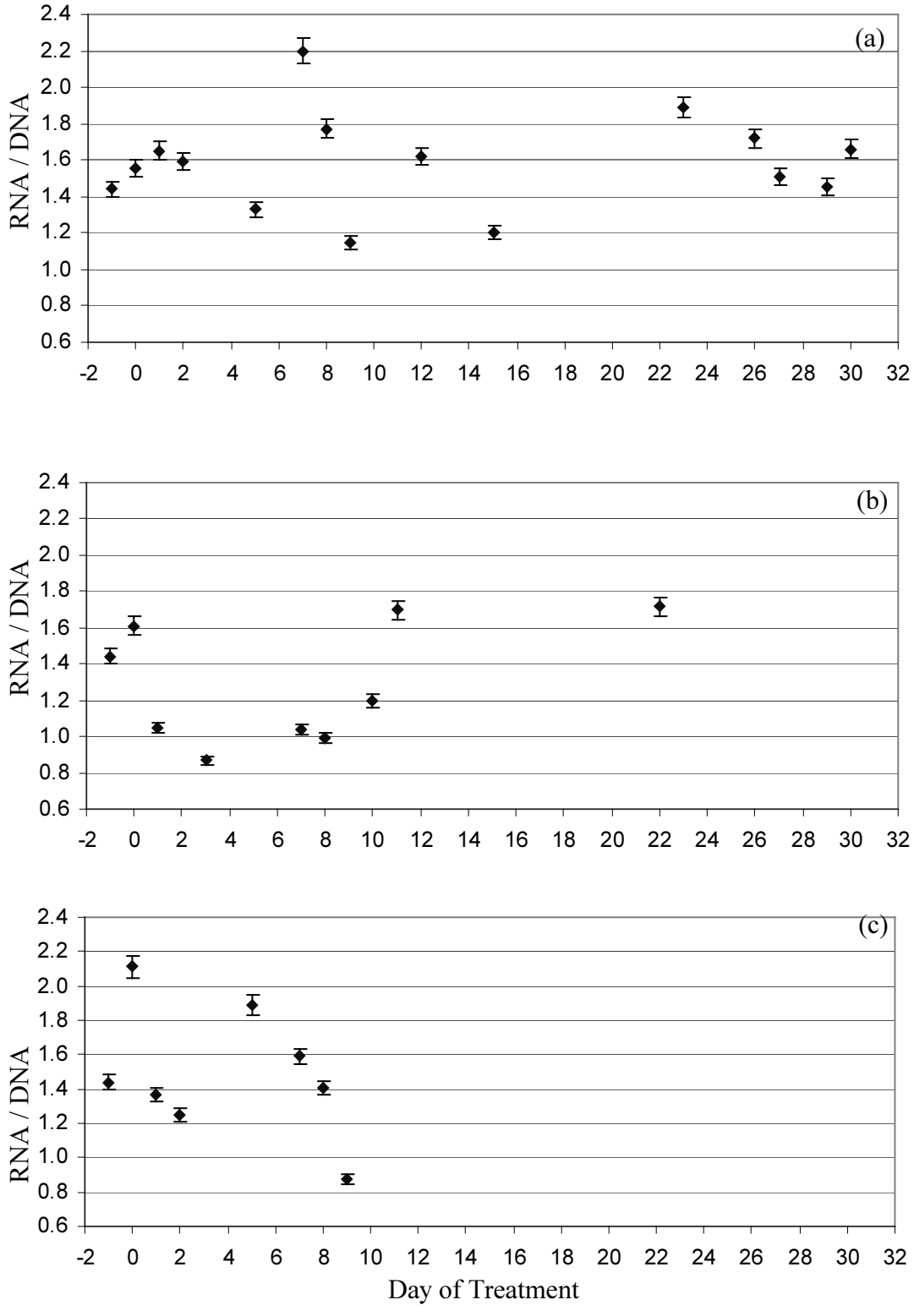

Fig. 5

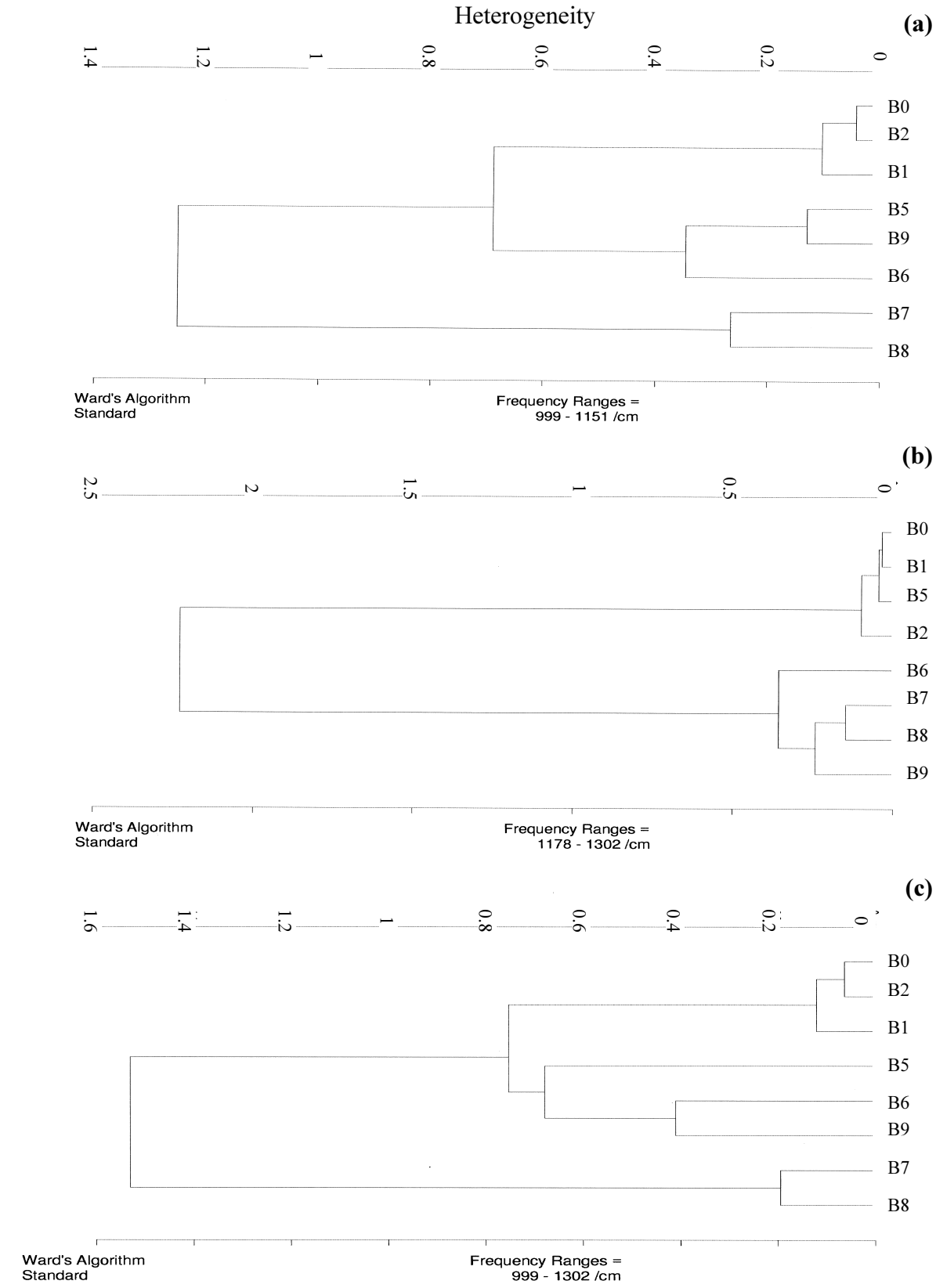
Heterogeneity
(a)
1.4
1.2
1
0.8
0.6
0.4
0.2
0
B0
B2
B1
B5
B9
B6
B7
B8
Ward's Algorithm
Standard
Frequency Ranges =
999 - 1151 /cm
(b)
2.5
2
1.5
1
0.5
0
B0
B1
B5
B2
B6
B7
B8
B9
Ward's Algorithm
Standard
Frequency Ranges =
1178 - 1302 /cm
(c)
1.6
1.4
1.2
1
0.8
0.6
0.4
0.2
0
B0
B2
B1
B5
B6
B9
B7
B8
Ward's Algorithm
Standard
Frequency Ranges =
999 - 1302 /cm

Fig. 6

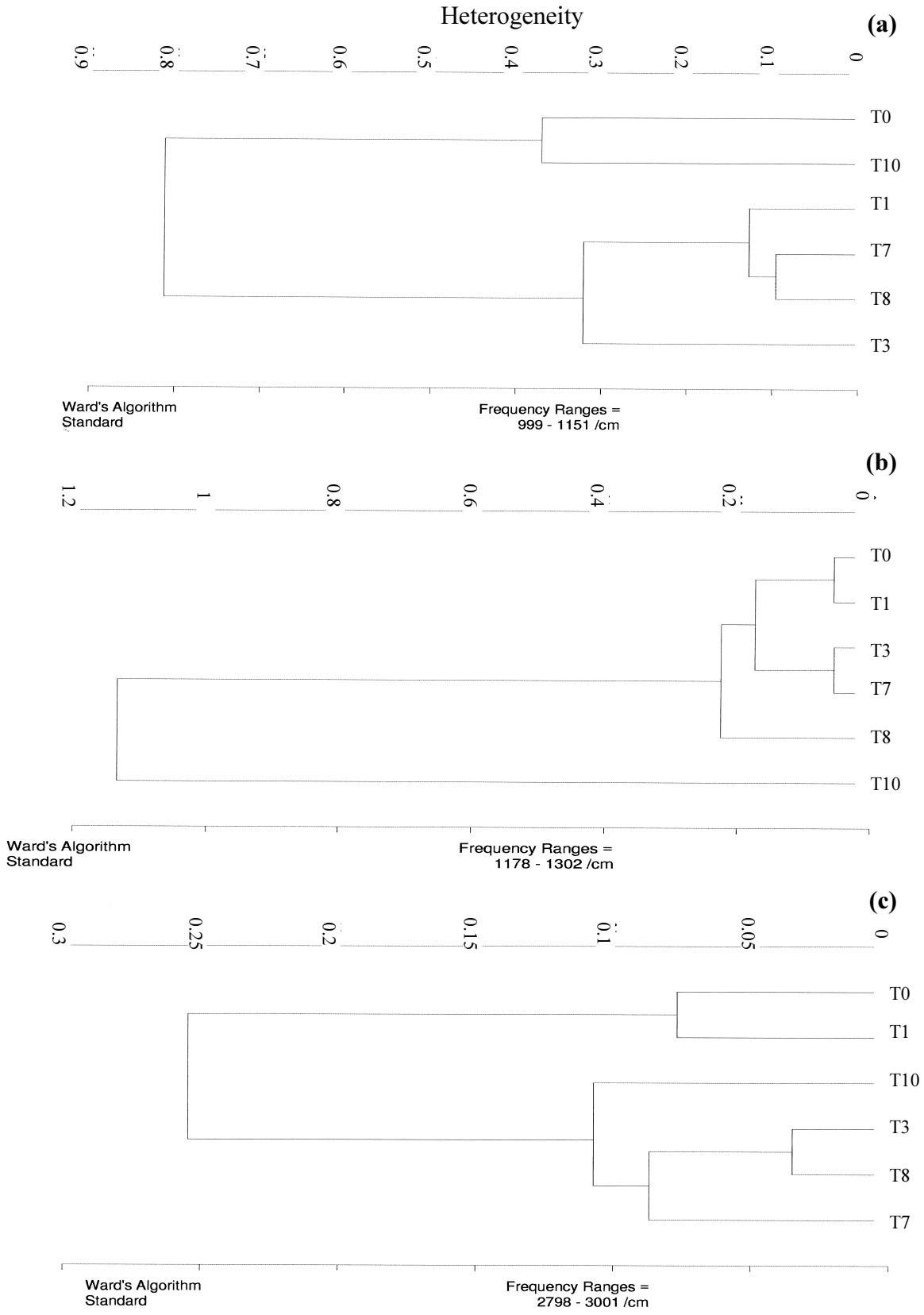
Heterogeneity
(a)
0.9
0.8
0.7
0.6
0.5
0.4
0.3
0.2
0.1
0
T0
T10
T1
T7
T8
T3
Ward's Algorithm
Standard
Frequency Ranges =
999 - 1151 /cm
(b)
1.2
1
0.8
0.6
0.4
0.2
0
T0
T1
T3
T7
T8
T10
Ward's Algorithm
Standard
Frequency Ranges =
1178 - 1302 /cm
(c)
0.3
0.25
0.2
0.15
0.1
0.05
0
T0
T1
T10
T3
T8
T7
Ward's Algorithm
Standard
Frequency Ranges =
2798 - 3001 /cm

Fig. 7

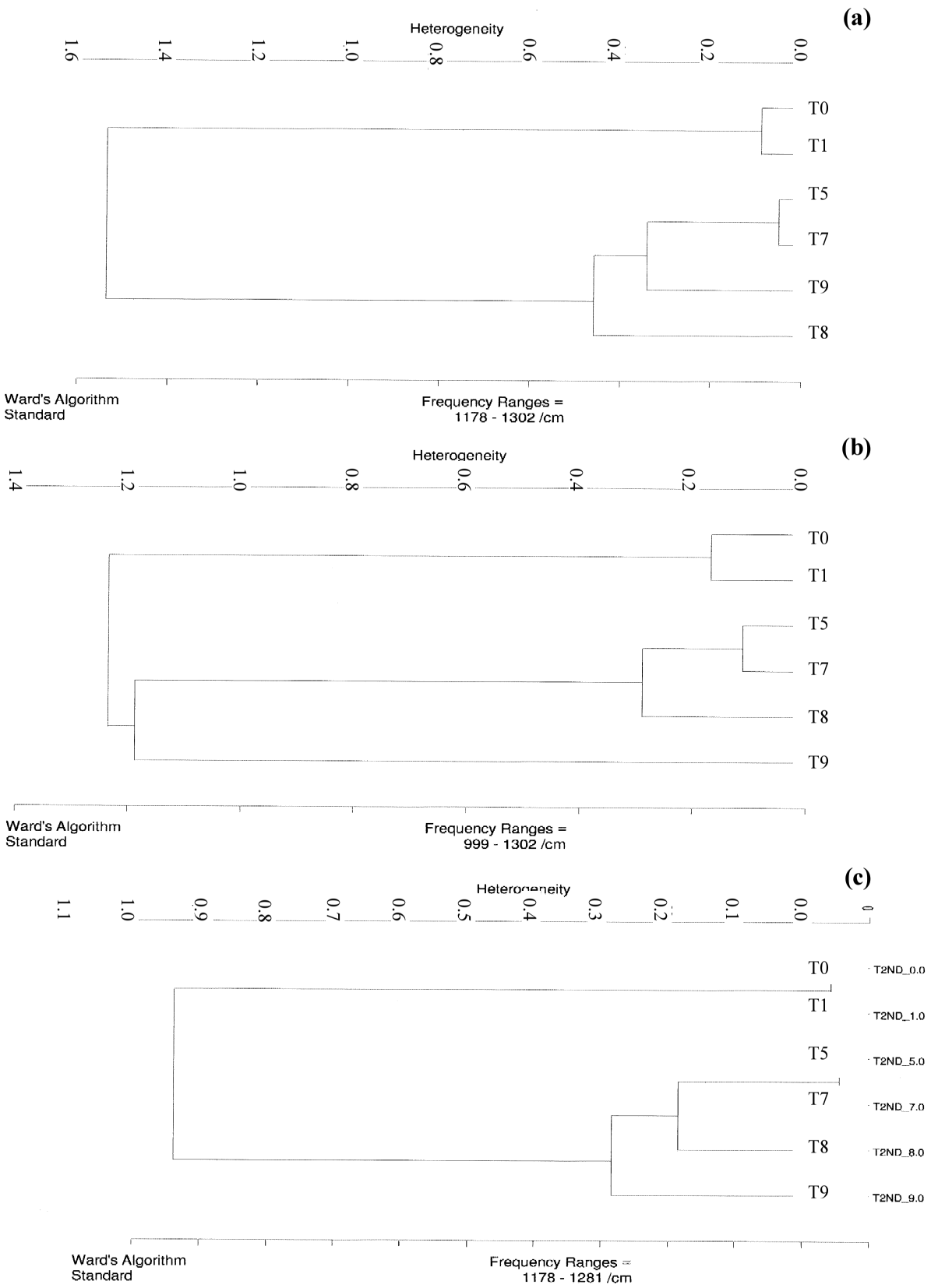
(a)
Heterogeneity
1.6
1.4
1.2
1.0
0.8
0.6
0.4
0.2
0.0
T0
T1
T5
T7
T9
T8
Ward's Algorithm
Standard
Frequency Ranges =
1178 - 1302 /cm
(b)
Heterogeneity
1.4
1.2
1.0
0.8
0.6
0.4
0.2
0.0
T0
T1
T5
T7
T8
T9
Ward's Algorithm
Standard
Frequency Ranges =
999 - 1302 /cm
(c)
Heterogeneity
1.1
1.0
0.9
0.8
0.7
0.6
0.5
0.4
0.3
0.2
0.1
0.0
T0
T1
T5
T7
T8
T9
T2ND_0.0
T2ND_1.0
T2ND_5.0
T2ND_7.0
T2ND_8.0
T2ND_9.0
Ward's Algorithm
Standard
Frequency Ranges =
1178 - 1281 /cm

Fig. 8